Magnetic moments and interactions near the metal-insulator transition in amorphous magnetic semiconductors

B. L. Zink,* V. Preisler, D. R. Queen, and F. Hellman
Department of Physics, University of California, San Diego, La Jolla, California 92093
(Received 14 July 2002; published 12 November 2002)

We report magnetization, magnetic susceptibility, and specific-heat measurements of amorphous $Gd_xY_ySi_{1-x-y}$ ternary alloy thin films near the metal-insulator (MI) transition as a function of temperature and applied magnetic field. Samples of the same magnetic moment concentration x but varying conduction-electron concentration $x+y$ were measured to test the effect of the MI transition on the magnetic properties. The effective moment in the paramagnetic state (per Gd atom) shows a strong dependence on composition, with a peak at the MI transition, independent of the Gd/Y ratio. Addition of Y weakens the Gd-Gd magnetic interactions, consistent with an indirect RKKY-like exchange interaction, despite the localized or nearly localized nature of the conduction electrons. Specific-heat measurements show further evidence of weakened RKKY-like interactions in the $y \neq 0$ sample via a spin-glass peak that is shifted to lower temperature, narrowed, and more field dependent.

DOI: 10.1103/PhysRevB.66.195208 PACS number(s): 75.40.Cx, 75.50.Lk, 75.50.Pp

I. INTRODUCTION

Previous magnetization measurements on amorphous Gd_xSi_{1-x} (a-Gd-Si) for compositions x near the metal-insulator (MI) transition show strong but balanced ferromagnetic and antiferromagnetic exchange interactions which suppress the magnetization well below the noninteracting Brillouin function and lead to a spin-glass freezing at temperatures below 10 K. This freezing shows many features of a classic spin glass including a split between zero field cooled and field cooled dc susceptibility and a weak but nonzero frequency dependence of the freezing temperature T_f ($\Delta T_f/T_f = 0.04$ per log decade change in frequency).[1,2]

In these alloys the susceptibility χ in the paramagnetic state above the spin-glass freezing is well described by a Curie-Weiss law:

$$\chi = A/(T-\theta) \tag{1}$$

with small θ ($\leqslant 2.5$ K and significantly below T_f for all x). The effective moment p in the paramagnetic state (from $A = n_{\mathrm{Gd}} p^2 \mu_B^2/3k_B$) shows a striking composition dependence, with a large peak at the MI transition and a significant suppression away from this composition. Related MI induced effects have been seen in magnetic measurements on crystalline P:Si, but with no spin glass-freezing, and the temperature dependence of susceptibility is not a Curie law.[3–6]

Gd is a $4f^7 5d^1 6s^2$ atom, virtually always trivalent. The Gd^{3+} ion has a large moment, $J=S=7/2$ and $L=0$, due to the half-filled f shell, hence single-ion anisotropy is negligible. The effective moment $p^2 = g^2 J(J+1)$ in the paramagnetic state is 7.9 μ_B. Because of the strongly local character of this large spin-only moment, Gd is not significantly affected by its environment, and exhibits values close to this ground-state moment ($7\mu_B$) and this effective moment ($7.9\mu_B$) in all known metallic and insulating alloys and compounds, with a possible exception observed by electron-spin resonance in Gd-doped SmB_6.[7] We have to date been unable to determine the saturation magnetization in a-Gd-Si, as M is not saturated even in fields as high as 25 T and still exhibits substantial susceptibility, indicating antiferromagnetic interactions of strength greater than 25 T (an energy scale equivalent to 120 K for $J=7/2$).[8]

The effective moment in the paramagnetic state in a-Gd-Si is however unambiguously not $7.9\mu_B$, instead dropping to as low as 5.5 μ_B, and is dependent on composition (up to $8\mu_B$ at the MI transition). We have speculated that two effects are influencing this effective moment: local moments associated with Si dangling bonds surrounding each Gd ion could be antiferromagnetically coupled to the Gd, acting to reduce the effective moment (and possibly contribute to the high-field susceptibility), and a paramagnetic (positive) contribution from conduction electrons in singly occupied localized states, which peaks at the MI transition as in P:Si. Note that the latter should not be visualized as localized on a single atomic site, but instead in a state with a finite localization length which will diverge at the MI transition and exceeds the interatomic distances even well into the insulating state.

Specific-heat measurements on a-Gd_xSi_{1-x} show large magnetic contributions at temperatures below 70 K, with a broad peak centered at $\approx 1.8\ T_f$, which is a common feature of spin glasses.[9–11] Near the MI transition these measurements also show magnetic entropies above the $S_{mag} = R\ln(2J_{\mathrm{Gd}}+1) = R\ln 8$ expected from Gd moments, suggesting that carriers localizing at the MI transition contribute local magnetic moments to the spin system. Theoretical studies of the amorphous rare-earth silicon alloys to date have focused on lattice polarons and the strong effect of the spin disorder on the carrier wave functions via a local moment-carrier exchange interaction[12,13] and have yet to explain many of the observed phenomena.

In metals such as crystalline Gd and $GdSi_2$, magnetism is mediated by an indirect Ruderman-Kittel-Kasuya-Yosida, (RKKY) exchange interaction between the Gd ions, which is ferromagnetic for Gd (Curie temperature $T_c = 293$ K) and antiferromagnetic for $GdSi_2$ (Néel temperature $T_N = 27$ K).

Direct exchange between Gd ions is expected to be negligible due to the local nature of the $4f$ electrons. Disorder alone does not fundamentally seem to change the nature of the interactions: a-Gd_xGe_{1-x} is ferromagnetic with $T_c > 150$ K for $x > 0.5$.[14] In the a-Gd-Si alloys, the electron concentration at the MI transition is not precisely known, but lies between 10^{20} cm^{-3} (from IR absorption measurements) and 10^{22} cm^{-3} (assuming trivalent Gd). The nature of the RKKY interaction in a strongly disordered high electron concentration system has not been theoretically studied, but near the MI transition in amorphous alloys, even on the insulating side, the localization length exceeds the inter-Gd distance and the electron concentration is high, hence an indirect conduction-electron-mediated RKKY-like exchange is the likely magnetic exchange mechanism. The effects of weak disorder have been studied;[15–17] early reports that the RKKY interaction would be exponentially damped with the mean free path were shown to be incorrect, and the primary effect of disorder was shown to be randomization of the phase of interaction. We have proposed that this randomization of phase might be the source of the nearly perfect balancing of ferromagnetic and antiferromagnetic interactions, which leads to the observed Curie law [$\theta = 0$ in Eq. (1)] despite the strength of the interactions.[2]

The purpose of the present work is to study the effect of adding conduction electrons to a-Gd-Si on the spin-glass behavior, specifically the magnetic interactions, effective moment, and magnetic entropy. Y is a $4d^15s^2$ atom, also virtually always trivalent and with the same size ionic radius as Gd but with no local moment. Addition of Y while holding constant the Gd concentration therefore has the effect of adding conduction electrons at constant local moment. Effects on the RKKY interaction of changing distance between moments have been frequently studied in metallic systems, but to our knowledge, the systematic study of the effects of changing electron concentration have been reported in only one other system. Varying carrier concentration causes dramatic changes in the magnetic properties of crystalline IV-VI semiconductors such as $Pb_{1-x-y}Sn_yMn_xTe$.[18–20] In these materials, as carrier concentration increases, the RKKY interaction at a fixed Mn-Mn distance changes sign, causing a change from ferromagnetism to spin-glass behavior. Though this system and our a-Gd-Y-Si have similarly large carrier concentration, the a-Gd-Y-Si adds the effects of strong disorder to the problem.

II. EXPERIMENT

Samples were made by electron-beam coevaporation under UHV conditions onto amorphous Si-N coated Si substrates and Si-N membrane based microcalorimeters which are held near room temperature during the deposition. We have previously described the design and use of these microcalorimeters in detail.[21,22] Structural characterization techniques including x-ray diffraction, transmission electron microscopy, and x-ray-absorption fine structure confirm that the samples are amorphous and show no measurable clustering of Gd or Y.

The Si-N coated Si substrates are used for magnetization measurements. The magnetization and specific-heat samples are therefore grown in the same depositions, allowing direct comparison. The microcalorimeters were fabricated from the same wafer, and have $\approx$2000-Å thick Al thermal conduction layers which were grown in the same thermal evaporation. Additional microcalorimeters from this batch were left with no samples deposited in order to measure the specific heat of addenda, C_{add}. This gives the lowest possible deviation in the thermal properties of the microcalorimeters, which aids in comparing the two magnetic samples. The compositions, Gd concentration (Gd atoms/cm^2), and areal density (total atoms/cm^2) were determined by Rutherford backscattering (RBS). The thicknesses of the samples were found using a Dektak profilometer. For magnetization measurements, the lateral area of the films on the Si-N substrates was measured by creating a high-resolution image of the sample with a digital scanner. This image is then analyzed using photomanipulation software, and the area of the substrate covered by the film measured to within several percent. The area of the films deposited on the microcalorimeters is determined by the size of the micromachined shadow mask used to define the deposition area.

The samples chosen for this study are an a-$Gd_{14}Si_{86}$ film and an a-$Gd_{14}Y_7Si_{79}$ film. The Gd-Si sample is very near the MI transition, with conductivity $\sigma < 10(\Omega\ \mathrm{cm})^{-1}$ at 4 K and a large effective moment.[2] The conductivity of the ternary film with 14% Gd and 7% Y is $> 500(\Omega\ \mathrm{cm})^{-1}$ at 4 K, placing it it well on the metallic side of the transition.[23]

Magnetization measurements were made using two Quantum Design superconducting quantum interference device magnetometers, one with a high-field superconducting magnet and a similar system optimized for low-field ac susceptometry. In both high-field dc and ac measurements, the temperature-independent background was determined from a measurement at 300 K. At this temperature the sample's χ is very small, $\ll \chi$ at low T.

In order to measure specific heat, the microcalorimeter is mounted in a sample-in-vacuum He^4 cryostat. This cryostat is compact and can be inserted into either a LHe storage dewar or into the bore of an 8-T superconducting solenoid. In this cryostat the sample may be cooled to ≈ 2 K by pumping condensed LHe in a small 1-K pot. The microcalorimeters use a-Nb_xSi_{1-x} resistive thermometers for measurements at low temperatures. Because small variations in the composition of these thermometers can cause their resistances to be large (several megaohms) at low temperatures, the devices can be difficult to measure at the lowest temperatures. The microcalorimeters for this study were measured from $\approx 3.7-90$ K. Measurements were taken using the small-ΔT relaxation method,[24] with $\Delta T \cong 1\%$. This method requires three separate measurements. The thermometers must be calibrated, meaning resistance vs T must be measured at each temperature. A measurement of the resistance change ΔR when a known amount of power P is applied to the sample is converted to ΔT using the measured calibration. The thermal conductance of the device is given by $\kappa = P/\Delta T$. Finally the sample's temperature is recorded as it relaxes back to the block temperature, T_0 from $T_0 + \Delta T$, and this single exponential decay is fit to give τ. The specific

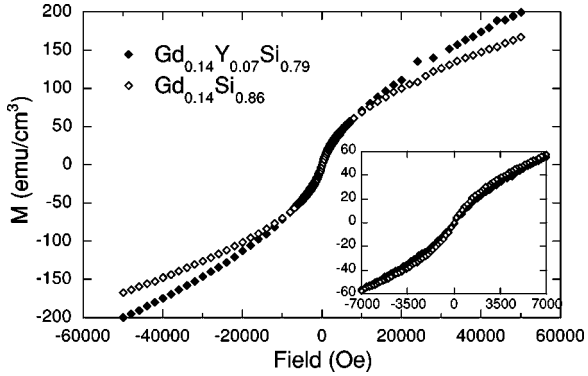

FIG. 1. Magnetization vs applied magnetic field at 4 K for both samples. Neither sample approaches saturation even at 50 000 Oe. They are also well below the Brillouin function, indicating strong antiferromagnetic interactions.

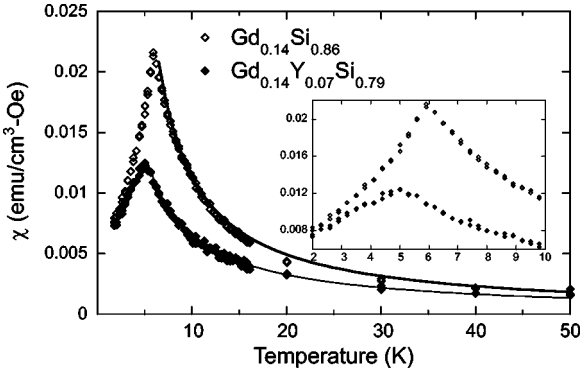

FIG. 2. χ_{ac} for *a*-Gd-Si and *a*-Gd-Y-Si samples as a function of temperature from 2 to 50 K. The cusps occur at the spin freezing temperatures T_f. Solid lines are Curie-Weiss fits to the data above T_f. Inset: The region near T_f.

heat is then $C=\kappa\tau$. Note that the measurement of κ requires an accurate calibration of R vs T, while the τ measurement is independent of this calibration.

III. RESULTS

Figure 1 shows $M(H)$ at 4 K for the $x=14, y=0$ and $x=14, y=7$ samples. Expected saturation magnetization values, assuming Gd^{3+} ions with $J=S=7/2$, are $M_{sat}=451$ emu/cm^{-3} for *a*-Gd-Si and $M_{sat}=456$ emu/cm^{-3} for the *a*-Gd-Y-Si. No hysteresis is seen above 1000 Oe for any sample at any temperature. All samples have magnetizations significantly below saturation and below the Brillouin function, with large high-field susceptibility, indicating strong antiferromagnetic interactions (since single-ion anisotropy and other contributions such as Van Vleck susceptibility should be negligible). With increasing temperature, $M(H)$ decreases for all samples, but $M(H,T)$ does not scale for any sample with H/T, as found previously for pure *a*-Gd-Si, also an indication of the importance of interactions. The expanded scale inset in Fig. 1 shows that the initial susceptibility is significantly larger for the pure *a*-Gd-Si sample ($y=0$, very near the MI transition) than for the $y=7$ sample (metallic), and that the data cross at about 10 000 Oe, above which the pure *a*-Gd-Si sample has lower magnetization and lower differential susceptibility $\partial M/\partial H$ than the ternary *a*-Gd-Y-Si sample. These two samples have virtually identical Gd concentrations (Gd atoms/cm^2 and total atoms/cm^2), as measured directly by RBS, and thicknesses (Gd atoms/cm^3).

Figure 2 shows the ac susceptibility $\chi(T)$ measured in zero dc field with 406-Hz ac field amplitude of 4 Oe and 5 Oe. Data taken in both fields collapse together, indicating that the low-field magnetization is linear in field. The *a*-Gd-Si sample shows the same classic spin freezing as previously measured, with the 406-Hz peak value in χ indicating a freezing temperature of $T_f=5.9$ K. The ternary sample shows a similar but smaller peak in χ at a lower temperature $T_f=5$ K. For both samples above T_f, in the paramagnetic state, χ is independent of frequency and has been fit with a Curie-Weiss law [Eq. (1)] shown as a solid line. It is clear even with no analysis that χ is drastically affected by the addition of Y; the susceptibility at all temperatures for $y=0$ is twice that of the $y=7$ sample. The Curie-Weiss law fits of the paramagnetic state above T_f show that A indeed is nearly doubled, indicative of an increase in the effective moment p by $\sqrt{2}$, as well as an increase in θ from approximately zero for $y=7$ (metallic) to 2.5 for $y=0$ (MI transition).

Figure 3 shows p vs overall composition $x+y$ for both samples in this paper, as well as the data from the earlier work on pure *a*-Gd_xSi_{1-x} ($y=0$) and *a*-Tb_xSi_{1-x}.[2,25] p is determined from the constant $A=n_{Gd}p^2\mu_B^2/3k_B$ in the Curie-Weiss fit shown in Fig. 2. Here n_{Gd} is the number of Gd atoms/cm^3. p is therefore measured in μ_B per Gd atom. The MI transition (based on electrical conductivity measurements[1,26,27]) is shown as a line at $x=14$. The effective moment p is largest at the MI transition and is suppressed on either side, independent of whether the shift in overall composition is due to changes in Gd or Y concentration.

The suppression in p from the expected values of 7.9 μ_B for Gd^{3+} and 9.7 μ_B for Tb^{3+} far from the MI transition is not understood at present, but we suggest that it is associated with a local polarization of antiferromagnetically coupled Si

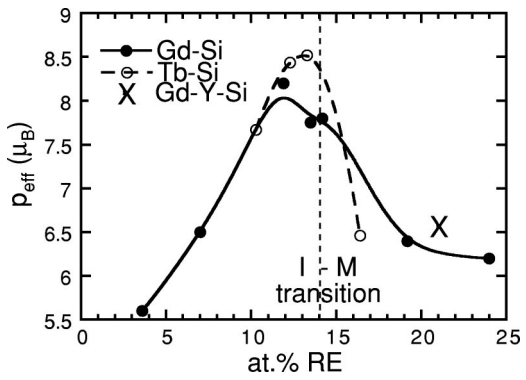

FIG. 3. Effective moment p as a function of metal ion content $x+y$ for several Rare-Earth–Silicon alloys. The peak occurs near the MI transition. The Gd-Si sample measured for this study has 13.5 at.% Gd. Lines are a guide to the eye.

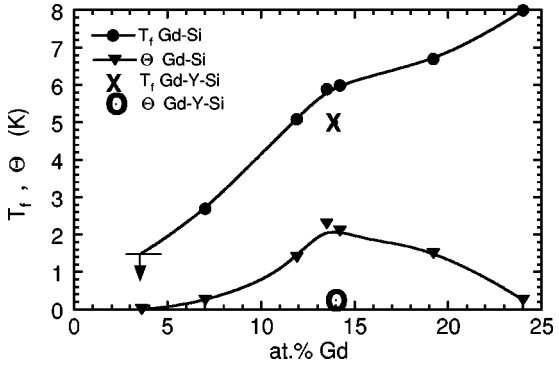

FIG. 4. The freezing temperature T_f and Curie-Weiss θ vs Gd concentration. The peak in θ and the near zero value found for the strongly metallic ternary sample (large solid circle) indicates the importance of the MI transition at 14 at.% Gd. The downward-pointing arrow indicates that 1.5 K is an upper limit on the freezing temperature of the 4 at.% Gd sample. Lines are a guide to the eye.

dangling-bond states surrounding each rare-earth ion; electron-spin-resonance measurements are underway to clarify this.

Figure 4 shows the freezing temperature T_f and θ versus Gd concentration. T_f is not significantly affected by the MI transition (it passes smoothly through, with a possible change in slope) but does increase with increasing Gd concentration, as is expected. T_f also decreases on adding Y for the same Gd concentration. θ shows the same peak at the MI transition as p.

Figure 5 shows the specific heat of the *a*-Gd-Si and *a*-Gd-Y-Si samples from ≈ 3 K up to 40 K, as well as an a-$Y_{21}Si_{79}$ sample. The units of specific heat in this plot are J/mol K, where a mole counts all atoms in the sample. We calculate the total number of atoms in each sample from the areal density, which is a direct result of the RBS measurements. Below T_f the specific heats of the two magnetic samples ($x \neq 0$) are nearly identical. As the temperature increases, *a*-Gd-Y-Si initially has a slightly larger specific heat, then falls well below that of *a*-Gd-Si. Both magnetic samples

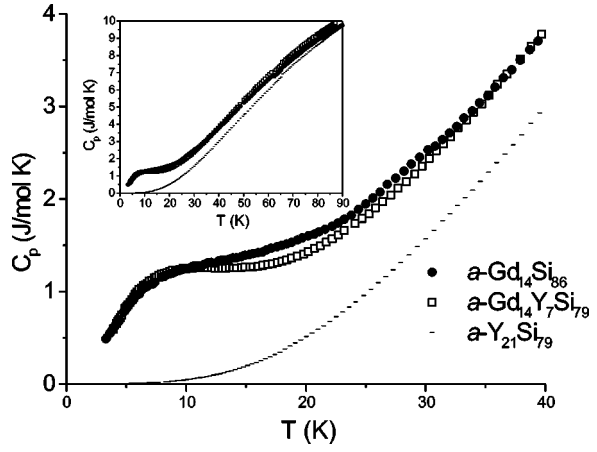

FIG. 5. The specific heat of a-$Gd_{14}Si_{86}$, a-$Gd_{14}Y_7Si_{21}$ and a-$Y_{21}Si_{79}$ samples in zero field. Inset: The same plot showing temperatures up to 90 K.

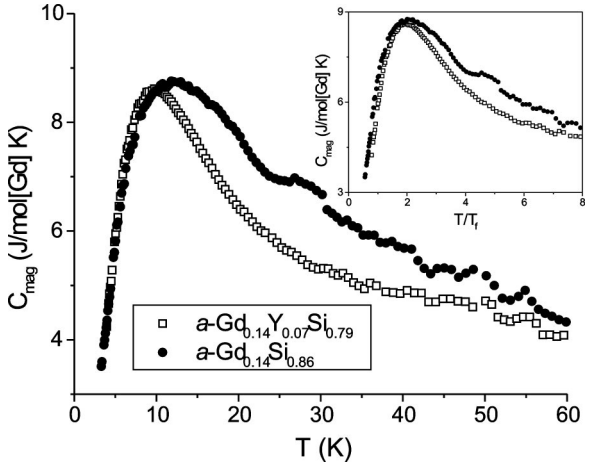

FIG. 6. Magnetic contribution C_{mag} vs T for $x=14, y=0$ and $x=14, y=7$ samples. Both show broad peaks above T_f commonly seen in spin glasses. The addition of Y causes a reduction of T_f causing the peak to shift to lower temperature. Inset: a C_{mag} vs T/T_f for the same samples shows that the peak occurs at $\approx 1.8T_f$ and that in the $y=7$ sample C_{mag} is smaller than the $y=0$ sample C_{mag} for $T/T_f < 8$.

have specific heats much larger than a-$Y_{21}Si_{79}$ at low temperatures. The inset in Fig. 5 shows the same samples up to 90 K. The specific heats of *a*-Y-Si and *a*-Gd-Si converge at the highest temperatures, while the ternary alloy has a C_p that is slightly larger than the other two samples, and larger than the *a*-Gd-Si sample above 40 K. Because the magnetic measurements described above and many aspects of the specific heat which will be detailed suggest that both the magnetic interactions and the effective moment are smaller in the *a*-Gd-Y-Si sample, it is unlikely that this additional specific heat is from an increased magnetic contribution, particularly since it is seen at 80–90 K. More likely, this larger C_p is a result of a small change in the phonon spectrum caused by the addition of the Y ions.

Figure 6 shows the estimated magnetic contribution to the specific heat C_{mag} for both magnetic samples in units of J/mol[Gd] K, meaning that the mole counts only Gd atoms in the samples. To determine C_{mag} we treat C_p as a sum of magnetic, electronic, and phonon contributions, $C_p = C_{mag} + C_{el} + C_{phon}$. Because yttrium and gadolinium have similar ionic radii and valences, we assume that C_{el} and C_{phon} are the same for *a*-Y-Si and *a*-Gd-Si samples of similar metal content. This is justified by their similar high-temperature C_p and is equivalent to assuming that *a*-Y-Si's specific heat has negligible C_{mag}. We estimate C_{mag} for the $y=0$ sample by subtracting a high-order polynomial fit to the a-$Y_{21}Si_{79}$ C_p from the measured C_p. Because the specific heats of a-$Y_{14}Si_{86}$ and a-$Y_{21}Si_{79}$ are very similar at all but rather low temperatures (<15 K) where both *a*-Y-Si films' C_p are much smaller than the magnetic samples, we simplify the analysis by using a-$Y_{21}Si_{79}$ for both magnetic alloys.[28]

Adding atoms to a material's unit cell commonly results in additional optical-phonon bands appearing in the dispersion relation. To estimate C_{mag} for the $y=7$ sample we must account for the slightly larger C_{phon} seen at higher tempera-

tures in Fig. 5. To do this we have added to the a-$Y_{21}Si_{79}$ data a contribution from an Einstein mode with $\theta_E = 150$ K, and $m = 0.018$ of the form

$$C_{Einstein} = 3mR(\theta_E/T)^2 \frac{e^{(\theta_E/T)}}{(e^{(\theta_E/T)}-1)^2}. \quad (2)$$

This term approximates the contribution to the specific heat from a soft optical mode. The values of θ_E and m were chosen so that the high-T data match in value and slope. We note that this $C_{Einstein}$ will be very small at low T, where the obvious contributions to C_{mag} dominate, and only becomes significant when the ternary sample's C_p begins to exceed that of pure a-Gd-Si.

The resulting C_{mag} shown for both samples in Fig. 6 is similar to that seen in typical spin-glass materials, with a broad peak centered at $\approx 1.8T_f$. This spin-glass peak is shifted to lower temperature by addition of Y, reflecting a shift in T_f, as expected from the magnetization results. The C_{mag} peak is also at a slightly lower value in a-Gd-Y-Si, and narrower than that seen in a-Gd-Si. Also note that C_{mag} for both samples converge at higher temperature (>60 K).

These points are reinforced by the C_{mag} vs T/T_f plot shown in the inset of Fig. 6. Here the temperature axis has been scaled by the value of T_f determined by the peak in the ac susceptibility (Fig. 2). This makes clear that the spin-glass peak occurs at $\approx 1.8T_f$ in both samples, and that the peak in the ternary alloy is narrower and smaller than the a-Gd-Si sample.

Figure 7 shows C_{mag} vs T from ≈ 3 K to 60 K for both samples in applied magnetic fields up to 8 T. These samples show behavior similar to both the previously measured a-Gd-Si samples and well-known spin glasses such as CuMn, with the specific heat reduced at low temperatures and increased at higher temperatures by applied magnetic field.[10,29] A unique feature of the a-Gd-Si samples is that applied fields cause shifts in C_p up to quite high temperatures, a result also apparent in Fig. 7. For both samples the 8 T data are measurably larger than those taken in zero field even at 60 K, which is at least 10 T_f.

Though the behavior of these two samples in applied field is qualitatively similar, the quantitative effects of applied field are rather different. Figure 7a shows that in an 8 T magnetic field, the a-Gd-Si's spin-glass peak is only slightly lowered and is broadened, but mostly retains its shape. The effect is that of the spin-glass peak shifting to higher temperatures. This is in contrast to the situation in a-Gd-Y-Si shown in Fig. 7(b), where at 8 T, the peak is significantly lower, and more broadened on the high-T side. This sample shows substantial field dependence at 4 T, and easily measurable shifts at 2 Tesla, though this data is omitted for clarity.

Figure 8 shows the field induced change in specific heat, $\Delta C = C(H=8\text{ T}) - C(H=0\text{ T})$ divided by $C(H=0\text{ T})$ as a function of scaled temperature T/T_f. The result is the relative change in specific heat at this field. Because we have previously confirmed that the thermal conductance κ of our microcalorimeter shows no field dependence[22] all the field dependence in our measurement appears in τ. Note therefore that

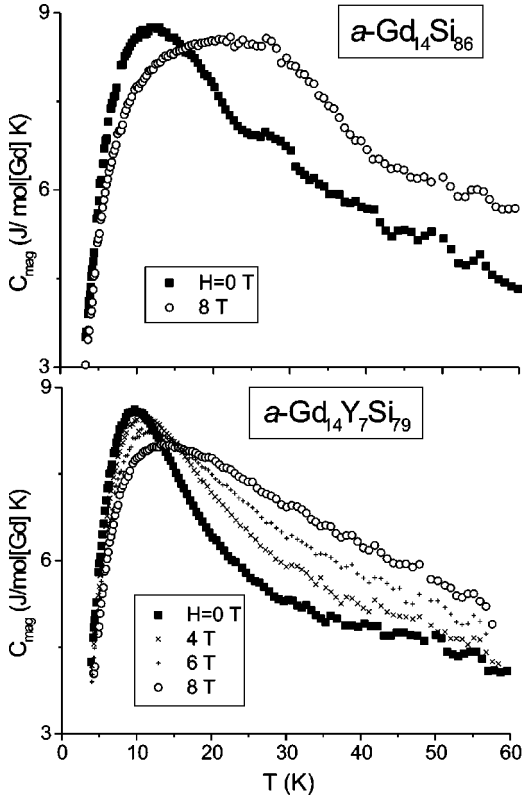

FIG. 7. Magnetic contribution to specific heat, C_{mag}, vs T for $y=0$ and $y=7$ samples in applied magnetic fields up to 8 Tesla. Applied field causes larger shifts in C_{mag} in the $y=7$ sample.

$$\frac{\Delta C}{C} = \frac{C_H - C_0}{C_0} = \frac{\kappa\tau_H - \kappa\tau_0}{\kappa\tau_0} = \frac{\Delta\tau}{\tau_0}. \quad (3)$$

This means that we obtain $\Delta C/C$ using only measurements of τ in high and zero field, with no possible influence from addenda or nonmagnetic analog subtractions or from fitting errors in the thermometer calibration required to calculate κ.

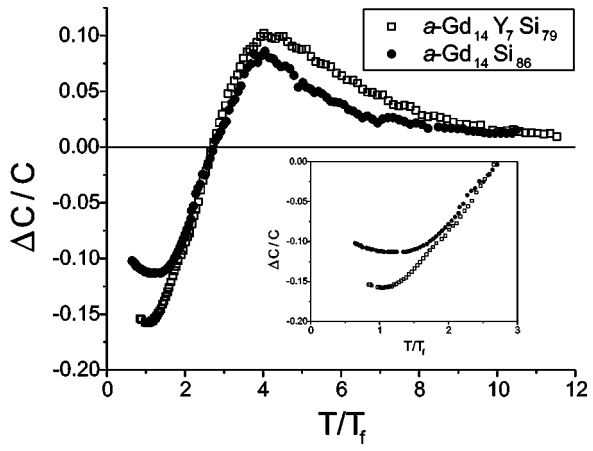

FIG. 8. Relative change in C_p at 8 T for both samples

TABLE I. Magnetic entropies and n [from Eq. 5] for the two samples. All entropies are in units of J/mol[Gd] K.

Sample	S_{mag} $(4<T<90$ K)	S_{excess} $[S_{mag}-R\ln(2J_{\mathrm{Gd}}+1)]$	n (localized e^-/Gd ion)	S_p $R\ln(2J_{eff}+1)$
$x=14$, $y=0$	20.0	2.7	3.9	17.1
$x=14$, $y=7$	18.5	1.2	1.7	15.7

This greatly simplifies the reduction of the data and makes this quantity the most accurate measure of field induced changes in C_p.

There are several interesting features apparent in Fig. 8. The simplest is that the data elegantly confirm the greater influence of magnetic field on the $y=7$ sample. $\Delta C/C$ is larger (either more negative or more positive) for the ternary sample for all T/T_f. Apart from the difference in magnitude, the two data sets have remarkably similar shapes. Both datasets have an apparent maximum negative value very near the freezing temperature ($T/T_f \approx 1.2$), both cross zero at $T/T_f \cong 2.7$, and both have a maximum positive value at $T/T_f \cong 4$ with tails extending out to at least $T/T_f = 10$. The inset shows the negative maximum near T_f. This negative maximum indicates that as temperature increases from the lowest measured temperatures to T_f, C_p is increasingly field dependent. At or slightly above T_f the field dependence begins to drop roughly linearly and at a common value of $T/T_f \cong 2.7$ for both these samples, $\Delta C/C = 0$, meaning that the specific heat at 0 and 8 T is the same. Then $\Delta C/C$ increases roughly linearly and peaks at $T/T_f \cong 4$ for both samples.

That any feature is seen at T_f is somewhat surprising, as none of the other high-field experiments, including magnetoresistance[1,26,27] and magnetization[2] have seen any feature near T_f in this material. Though this feature has thus far not been reported for other spin glasses, it is confirmed by data on other *a*-Gd-Si films.[10]

Table I shows measured and expected values of magnetic entropy for both $y=0$ and $y=7$ samples. The magnetic entropy S_{mag} is given by

$$S_{mag} = \int_{T=0}^{T_{max}} \frac{C_{mag}}{T} dT, \tag{4}$$

hence the area under the curve in a C_{mag}/T vs T plot gives the measured S_{mag} for a particular temperature range. The S_{mag} values that appear in Table I are determined by plotting C_{mag}/T vs T in zero field for each sample and numerically integrating over the temperature range 3.99 K$<T<$88 K. S_{mag} is significantly larger for the pure *a*-Gd-Si sample, and both samples have larger entropy than is expected from Gd ions alone ($S_{\mathrm{Gd}} = R\ln(2J+1) = R\ln 8 = 17.3$ J/mol[Gd] K). Because the lower limit of these measurements is 3.99 K, these S_{mag} values in fact underestimate the magnetic entropy because C_{mag} continues to lower temperatures. The entropies S_{excess} are the results of subtracting the Gd ion entropy from the measured entropy. Note that the $y=0$ sample's S_{excess} is roughly twice that of the $y=7$ sample. We have previously suggested that S_{excess} is the contribution from localized electrons in singly occupied states.[9] We therefore write the maximum magnetic entropy of a collection of Gd moments ($J_{\mathrm{Gd}} = 7/2$) and n localized electron moments per Gd ion ($s_e = 1/2$) as

$$S_{mag} = R[\ln(2J_{\mathrm{Gd}}+1) + n\ln(2s_e+1)]. \tag{5}$$

n, the number of localized electrons per Gd ion, may be calculated and the results appear in Table I. Note that n is also roughly a factor of 2 larger in the $y=0$ sample.

A slightly different approach to the magnetic entropy is to first calculate the effective spin J_{eff} from the values of p shown in Fig. 3 from $p^2 = g^2 J_{eff}(J_{eff}+1)$, where g is the Lande g-factor and is assumed to still be $g=2$. Then values of S_p are then calculated from $S_p = R\ln(2J_{eff}+1)$. Note that $S_{mag} - S_p \approx 3$ J/mol[Gd] K for both $y=0$ and $y=7$ samples.

IV. DISCUSSION

The effect of increasing electron concentration on the magnetic interactions is very clearly seen in the changes in both $M(H)$ for the $x=14$ pair shown in Fig. 1 and in the magnetic susceptibility $\chi(T)$ shown in Fig. 2. The increased effective moment of the $y=0$ sample is visible in the lower-field $M(H)$ data, where $y=0$ has larger values (Fig. 1, inset) than $y=7$, and is dramatically seen in the factor of 2 difference in χ. At higher fields, the crossing of the data directly reflects the reduced interaction strength for the $y=7$ sample caused by increasing electron concentration. Since the Brillouin function represents $M(H,T)$ for noninteracting moments, suppression below this means antiferromagnetic interactions; the increased values of M at high fields for the ternary sample ($y=7$) therefore reflect a *reduction* in the strength of the antiferromagnetic interactions, consistent with the reduced freezing temperature T_f and θ in the $y=7$ sample relative to the $y=0$ sample, shown in Fig. 4. We note again that these two samples have been shown by RBS to possess identical Gd concentrations and inter-Gd distances (within the accuracy of RBS, which is $\approx 1\%$). Because the magnitude of the RKKY interaction goes as $(1/k_F R)^3$, a reduction in interaction strength with increasing electron concentration is consistent with an RKKY-like conduction-electron-mediated exchange, assuming a constant nearest-neighbor Gd-Gd distance R. This is a slightly different result than observed in the $Pb_{1-x-y}Sn_yMn_xTe$, where the carrier induced ferromagnet to spin-glass transition is caused by a change in the sign of the RKKY interaction due to increased k_F. It is likely that the presence of strong disorder and resulting randomization of the phase of the interaction prevents such a well-defined transition from occurring in our system.

In the presence of strong frustrated interactions such as are found here, it is not clear that the Curie-Weiss mean-field approach [Eq. (1)] is the correct physics for the paramagnetic state above T_f. We note however that the peaks in p and θ at the MI transition are both associated with an increased χ, which is the essential physics. Also, θ is quite small [relative to both the freezing temperature and the strength of the interactions as manifested by the high-field $M(H)$ suppression below the Brillouin function and the high-field susceptibility]. We note that in metallic Gd glasses, θ usually greatly exceeds the freezing temperature (typical $\theta > 25$ K for $T_f \approx 5$ K). In the present samples, the near zero value of θ, despite the clear presence of strong antiferromagnetic interactions, shows again the nearly perfect balancing of ferromagnetic and antiferromagnetic interactions, which we suggest is a consequence of the disorder-induced phase randomization of the RKKY interaction.[15–17] We suggest that the key elements for this near perfect balancing of strong interactions are strong disorder and lower electron concentration than the usual RKKY glasses (hence longer interaction range).

Several features of the magnetic contribution to the specific heat, $C_{mag}(T)$, also point to strong, balanced, long-range RKKY-like interactions, with weaker interactions in the $y=7$ sample. C_{mag} provides information on the density of magnetic states in these materials, and thereby the distribution of interaction strengths present in these spin glasses. The large peaks in C_{mag} for both samples at $\approx 1.8T_f$ indicate the large number of nearly degenerate magnetic states with energies close to T_f. The fact that adding conduction electrons to the system causes the spin-glass peak in C_{mag} to be lower in value and narrower means that there are fewer magnetic states near T_f, with a narrower distribution in energy. This result is of course also clear from the S_{mag} values which are much lower for $y=7$, and is expected from an RKKY-like interaction with an increased electron concentration.

The difference between the magnetic specific heats for the two samples is less dramatic than that observed in the susceptibility. This follows a pattern also observed in crystalline phosphorus-doped silicon (P:Si), where measurements of χ showed large differences across the MI transition as electrons localized into singly occupied states, while C_p showed more subtle effects.[3,4,30] This is expected, as χ measures the fluctuations of magnetic moments in response to an applied field and is therefore sensitive to the total number of localized moments n. $C_{mag}(T)$ depends on the density of magnetic states, and therefore dn/dT. Integrating to determine S_{mag} returns the emphasis to the total number of magnetic states, and in our measurements the difference between $S_{excess} = S_{mag} - R \ln 8$ for the two samples (and the resulting difference in n) is approximately a factor of two, similar to the change seen in χ. The difference in the field dependence of C_{mag} for these 2 samples is similarly dramatic, which again indicates weaker interactions and recalls the different field dependences of $M(H)$ for the two samples.

Another interesting result is the fact that for both these samples C_{mag} and $\Delta C/C$ persist to temperatures as high as $T/T_f \cong 13$ ($T \approx 80$ K) and are of similar value at these temperatures. This suggests that the strongest interactions in the distribution are less affected by moving away from the MI transition. This temperature range is also the same as that over which the *a*-Gd-Si demonstrates measurable magnetoresistance.[1] Such a link between the specific heat and electron transport is unique and suggests a need for further study.

V. CONCLUSIONS

In summary, we have shown that the susceptibility of amorphous Gd-Si alloys has a strong peak (a factor of 2) at the MI transition, independent of whether the MI transition is caused by increasing magnetic Gd content or nonmagnetic Y content. This peak in susceptibility can be described in terms of an increased effective moment. The magnetic contribution to specific heat shows spin-glass peaks near $T/T_f \cong 1.8$, with the metallic ($y=7$) sample showing a smaller, more field-dependent C_{mag}. Both samples have measurable C_{mag} as high as $T/Tf \cong 13$, $T \approx 80$ K, the temperature at which negative magnetoresistance becomes measurable in these samples.

We have also shown through measurements of both magnetic susceptibility and specific heat that the magnetic interactions in amorphous Gd-Si alloys are strong, of mixed sign (nearly perfectly balanced ferromagnetic and antiferromagnetic) and are reduced in absolute magnitude by the addition of Y (while maintaining the Gd-Gd distance and concentration constant). We suggest that the latter observation is consistent with an RKKY-like indirect exchange mediated by conduction electrons, despite the conduction electrons nearly being localized, in that increasing electron concentration reduces the strength of the interaction at a given distance.

ACKNOWLEDGMENTS

We would like to thank M. Liu for valuable discussions, S. Pfeil and M. Liu for help with data collection, CIMS at UCSD for the use of the magnetometer, Ami Berkowitz for the use of the superconducting magnet system, Bob Culbertson for RBS analysis, and the NSF for support.

*Electronic address: barry@physics. ucsd. edu

[1] F. Hellman, M.Q. Tran, A.E. Gebala, E.M. Wilcox, and R.C. Dynes, Phys. Rev. Lett. **77**, 4652 (1996).
[2] F. Hellman, D.R. Queen, R.M. Potok, and B.L. Zink, Phys. Rev. Lett. **84**, 5411 (2000).
[3] A. Roy and M.P. Sarachik, Phys. Rev. B **37**, 5531 (1988).
[4] A. Roy, M. Turner, and M.P. Sarachik, Phys. Rev. B **37**, 5522 (1988).
[5] R.N. Bhatt and P.A. Lee, Phys. Rev. Lett. **48**, 344 (1982).
[6] R.N. Bhatt, Phys. Scr., T **14**, 7 (1986).
[7] G. Wiese, H. Schaffer, and B. Elschner, Europhys. Lett. **11**, 791 (1990).
[8] F. Hellman, W. Geerts, and B. Donehew (unpublished).
[9] B.L. Zink, E. Janod, K. Allen, and F. Hellman, Phys. Rev. Lett. **83**, 2266 (1999).
[10] B. L. Zink, E. Janod, R. Sappey, and F. Hellman, (unpublished).

[11] J. A. Mydosh, *Spin Glasses: An Experimental Introduction* (Taylor and Francis, London, 1993).
[12] S. Kumar and P. Majumdar, Int. J. Mod. Phys. B **15**, 2683 (2001).
[13] A. M. Bratkovsky, in *Vibronic Interations: Jahn-Teller Effect in Crystals and Molecules*, edited by M. D. Kaplan and G. O. Zimmerman (Kluwer, Netherlands, 2001), pp. 133–140.
[14] R.J. Gambino and T.R. McGuire, IEEE Trans. Magn. **MAG-19**, 1952 (1983).
[15] P.F. de Chatel, J. Magn. Magn. Mater. **23**, 28 (1981).
[16] K.M. Wong and S.J. Poon, J. Magn. Magn. Mater. **42**, 130 (1984).
[17] A. Jagannathan, E. Abrahams, and M.J. Stephen, Phys. Rev. B **37**, 436 (1988).
[18] T. Story, P.J.T. Eggenkamp, C.H.W. Swuste, H.J.M. Swagetn, W.J.M. de Jonge, and L.F. Lemmens, Phys. Rev. B **45**, 1660 (1992).
[19] W.J.M. de Jonge, T. Story, H.J.M. Swagten, and P.J.T. Eggenkamp, Europhys. Lett. **17**, 631 (1992).
[20] C.W.H.M. Vennix, E. Frikkee, P.J.T. Eggenkamp, H.J.M. Swagten, K. Kopinga, and W.J.M. de Jonge, Phys. Rev. B **48**, 3770 (1993).
[21] D.W. Denlinger, E.N. Abarra, K. Allen, P.W. Rooney, M.T. Messer, S.K. Watson, and F. Hellman, Rev. Sci. Instrum. **65**, 946 (1994).
[22] B.L. Zink, B. Revaz, R. Sappey, and F. Hellman, Rev. Sci. Instrum. **73**, 1841 (2002).
[23] J. J. Cherry and F. Hellman, (unpublished).
[24] R. Bachman, F.J. DiSalvo Jr., T.H. Geballe, R.L. Green, R.E. Howard, C.N. King, H.C. Kirsch, K.N. Lee, R.E. Schwall, H.-U. Thomas, and R.B. Zubeck, Rev. Sci. Instrum. **43**, 205 (1972).
[25] M. Liu and F. Hellman (unpublished).
[26] P. Xiong, B.L. Zink, S.I. Applebaum, F. Hellman, and R.C. Dynes, Phys. Rev. B **59**, R3929 (1999).
[27] W. Teizer, R.C. Dynes, and F. Hellman, Solid State Commun. **114**, 81 (2000).
[28] B. L. Zink and F. Hellman (unpublished).
[29] L.E. Wenger and P.H. Keesom, Phys. Rev. B **13**, 4053 (1976).
[30] M. Lakner, H.v. Löhneysen, A. Langenfeld, and P. Wölfle, Phys. Rev. B **50**, 17 064 (1994).